Head loss coefficient through sharp-edged orifices

Nicolas J. Adam, Giovanni De Cesare and Anton J. Schleiss
Laboratory of Hydraulic Constructions, Ecole Polytechnique fédérale de Lausanne, Lausanne, Switzerland

E-mail: nicolasjean.adam@epfl.ch

Sylvain Richard, Cécile Muench-Alligné
Institut de système civil,HES SO Valais Wallis, Sion, Switzerland

Abstract. Nowadays, high-head power plants could increase their installed power capacity for many reasons, e.g. dam heightening, increase of their peak power capacity or refurbishment with new turbines. Frequently, due to several considerations, e.g. topographical or economical limitations, the existing surge tank cannot be extended to keep previous safety levels and efficiency. A valuable way to adapt these surge tanks is to place a throttle at their entrance like, for example, an orifice. The main effect of this adaptation is the introduction of head losses that reduce the extreme levels in the surge tank due to the mass oscillations resulting from a closure or opening of downstream discharge control.

This research studies the influence of the edge angle of a ASME-standard orifice on the head losses. This angle introduces an asymmetrical behavior and influences head losses. Different angles are tested from 0° to the 67° (biggest angle possible for this configuration). The first step of this study is to determine experimentally the steady losses produced by orifice for several discharges. In the second step, a numerical model on ANSYS CFX is performed.

Combining the two approaches, it is possible to understand and quantify the effect of the edge angle.

1. Introduction

Surge tank orifices allow introducing head losses between a surge tank and the waterway. The introduction of an orifice allows the reduction of extreme water levels in the tank and, by extension, to keep the same surge tank geometry during a refurbishment (increase of discharge). Refurbishments enable to increase power generation of hydroelectric power plants in order to improve their ability to produce large amount of electricity in short laps of time.

During the study of a hydroelectric plant refurbishment [1], the first step is generally to simulate the whole waterway with a 1-dimensionnal transient model using either the method of characteristics [2] or a similitude between hydraulic behavior and elements with electrical ones [3]. The results of this step are actually values of head loss coefficients in both directions, i.e. flowing in and out the surge tank. In some cases, these coefficient might be different by introducing a high asymmetry. Due to a lack of knowledge of the effect of orifice geometry on head losses, the geometries producing head losses are usually evaluated case-by-case with a physical model [1].

This study focuses on standard orifice shapes [4] and assesses the effect of the angle variation on asymmetricity and head losses in both directions. The first part of the study performs

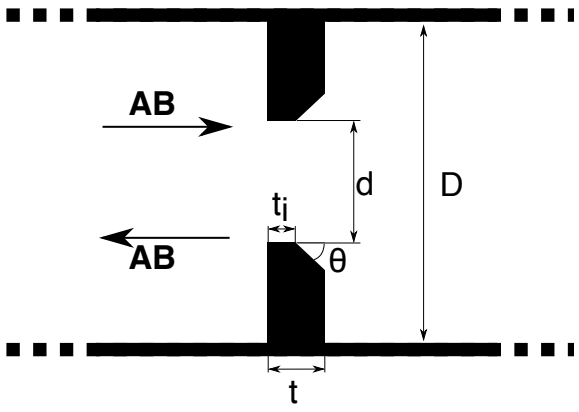

Figure 1. Orifice geometry

Table 1. Tested orifices with contraction ratio, thickness ratio, inner thickness ratio and sharp-edged angle

Orifice	β [−]	α [−]	α_i [−]	θ [deg]
1	0.5	0.2	0.1	0
2	0.5	0.2	0.1	15
3	0.5	0.2	0.1	30
4	0.5	0.2	0.1	45
5	0.5	0.2	0.1	67

experiments on physical set-up. Then, the second part compares physical results with performed simulations on numerical set-up.

2. Tested orifices

This study focuses on the influence of the sharp-edged angle, θ (Figure 1) on head losses in both directions. Even if the reference orifice geometry comes from a standard definition of orifice flowmeters [4], the orifice thickness is higher: $\alpha = 0.2$ instead of smaller than $\alpha < 0.05$. Each orifice geometry (Figure 1) can be characterized by four dimensionless numbers (Table 1) as shown below:

- $\beta = \frac{d}{D}$, the orifice diameter ratio,
- $\alpha = \frac{t}{D}$, the orifice thickness ratio,
- $\alpha_i = \frac{t_i}{D}$, the inner orifice thickness ratio,
- θ, the sharp-edged angle.

In this study, only the effects introduced by the angle are evaluated. Five angles are tested from 0° (rectangular shape) to 67° (highest possible angle). All geometrical characteristics of the tested orifices are shown in Table 1.

3. Physical set-up

The physical set-up (Figure 2) takes place in the Laboratory of Hydraulic Constructions (LCH) in Lausanne. The main pipe, where orifices are tested, has an inner diameter D of $0.216\,m$ and a length of $4\,m$ while the water supply and restitution of the set-up have a diameter of $0.150\,m$.

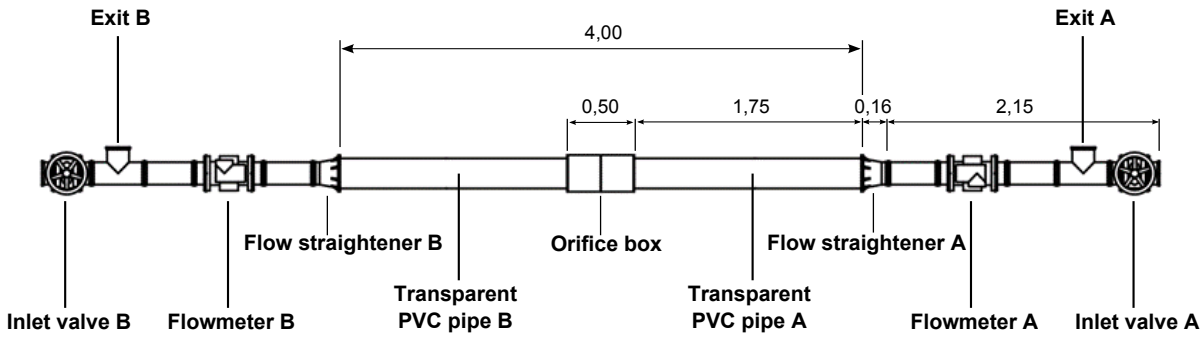

Figure 2. Physical set-up at LCH

Head losses are evaluated in both flow directions (from inlet A to exit B and from inlet B to exit A). For each direction, one flowmeter, A or B, records the discharge flowing in the set-up with an electromagnetic flowmeter (Endress-Hauser PROMAG 50W).

Furthermore, there are 12 sections on each transparent PVC pipe where the pressure is recorded. The pressure is recorded by piezoresistive pressure sensors averaged on 4 points equally placed over the perimeter (the highest, lowest, most left and right points).

4. Numerical set-up

The simulated numerical domain is only composed by both transparent PVC pipes and orifice box (Figure 2). In other words, the numerical set-up is a 4-meters pipe with a diameter of 0.216m and orifice placed at the middle section.

Numerical simulations are performed using the flow solver ANSYS-CFX version 15.0 to evaluate local head losses produced by the orifice. The used closing turbulence model is the $k - \Omega$ model.

The computational domain is discretized on an unstructured mesh of 3,8 million elements composed by tetrahedrons (Figure 3). The initial time step is 10^{-3}s. This time step is automatically adapted to insure a RMS CFL smaller than 5. Furthermore, to solve properly the boundary layers close to walls, a wall function approach is used instead of near wall approach which requires very fine meshes near the wall. The well functioning of the wall function approach is ensured if the dimensionless distance to the wall of the first node, y^+ is between 30 and 300. Furthermore, a non-slip wall condition is used with the PVC pipe roughness.

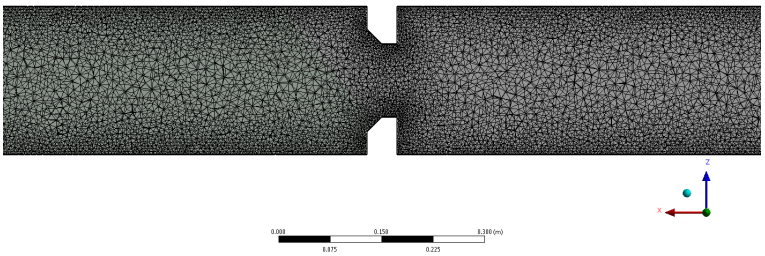

Figure 3. Local view of the mesh composed by tetrahedrons

Table 2. Set of discharge, kinetic energy and the Reynolds number in the main pipe

$Q\,[l/s]$	$K\,[m]$	$Re_P\,[-]$
0	0	
9.5	0.003	$5.6 \cdot 10^4$
13.4	0.007	$7.9 \cdot 10^4$
16.4	0.010	$9.7 \cdot 10^4$
19.0	0.014	$11.2 \cdot 10^4$
21.2	0.017	$12.5 \cdot 10^4$
23.2	0.020	$13.7 \cdot 10^4$
25.1	0.024	$14.8 \cdot 10^4$
26.8	0.027	$15.8 \cdot 10^4$
28.5	0.031	$16.8 \cdot 10^4$
30.0	0.034	$17.7 \cdot 10^4$

In this study, simulations are performed only for the highest discharge (Table 2). The simulation domain represents only the main pipe with a diameter of $0.216\,m$ (PVC Pipe A + B and orifice box in Figure 2). The inlet boundary condition is an upstream velocity condition equal to the uniform velocity for the highest tested discharge on the physical set-up($U = 0.819\,m/s$). At the outlet, an average constant relative pressure equal to $0\,Pa$ is imposed. The main target is the evaluation of head losses and of the pressure upstream to the orifice.

5. Methods

5.1. Physical experiments

For each orifice described in section 2, head losses are evaluated two times for a set of ten discharges (Table 2). The lowest Reynold number in the main pipe is higher than 10^4 to insure a fully turbulent behaviour [5, 6]. The kinetic energy in the main pipe varies from $0.003\,[m]$ to $0.034\,[m]$.

For each test, pressures and discharges are recorded during $30\,s$ with a sampling frequency of $100\,Hz$. Then, average pressures are evaluated at 24 control sections. Head losses are found by applying Bernoulli's law (Eq.(1))between upstream and downstream head (orifice point of view). Thus, the pressure along the main pipe is known except in the orifice box where there is no pressure sensor.

$$Z_{up.} + \frac{v_{up.}^2}{2g} + \frac{p_{up.}}{\rho g} = Z_{dn.} + \frac{v_{dn.}^2}{2g} + \frac{p_{dn.}}{\rho g} + \Delta H \tag{1}$$

where Z is the elevation in $[ma.s.l.]$ of a given point or section, v is the velocity at a given point or flowing through a given section in $[m/s]$, p is the pressure at a given point or section in $[N/m^2]$, ρ the water density in $[kg/m^3]$ and ΔH is the head loss between two sections.

Figure 4 shows schematically the principle of head losses evaluation for a given discharge. There are two averaging zones, one upstream and another downstream, to determine local head losses produced by the tested orifice. The downstream averaging zone must be further away than recirculation zones (taking place from 0 to $3.15\,D$ downstream of the orifice according to [7]).

The determination of the head loss coefficient can be found as shown in Eq.2. Linear head losses, which are produced by viscosity and pipe wall roughness, are assumed small enough to

be neglected in this study. For the highest discharge and in the upstream averaging zone, the linear head losses are equal to $0.001\,m$ which is a physical limitation. Also, velocity correction factors are neglected in the Bernoulli's law and the relation between head losses as well as kinetic energy (see Eq.(1) and (2)).

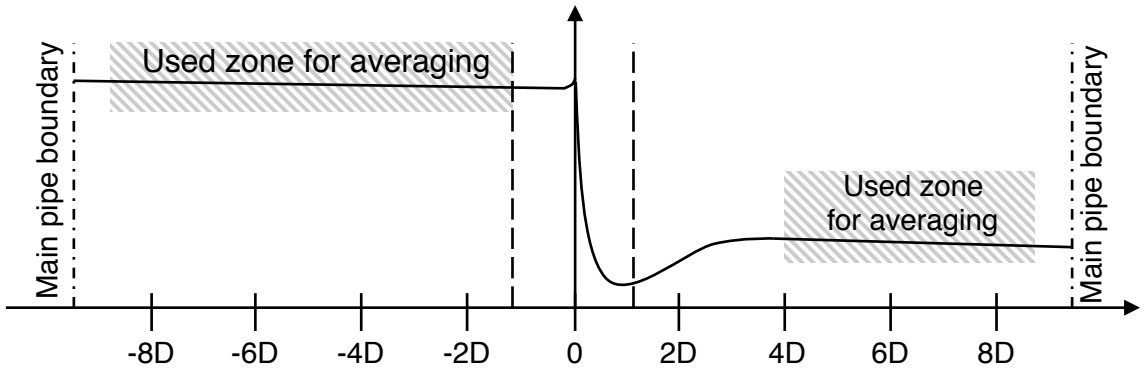

Figure 4. Principle of head losses determination (Orifice position is at 0)

$$\Delta H = k \cdot \frac{v^2}{2g} \tag{2}$$

where ΔH are the head losses in $[m]$, k the head loss coefficient relative to the reference section (here, equals to pipe area), v the velocity in the reference section, g the gravitational acceleration.

5.2. Numerical experiments

Steady numerical simulations are performed. The convergence criteria is defined as pressure fluctuations between two following time steps are smaller than $0.001\,m$. The numerical results, for orifices described in Table 1, are performed to compare with experimental ones. A comparison between the pressure averaged over the whole section and the 4-points averaged pressure on the perimeter were performed and the differences are small. Thus, only 4-points averaged pressure on the perimeter are used in the analysis.

6. Results

6.1. Physical

Figure 5 shows the average pressure for the 24 control sections along the pipe. Downstream pressure is set to 0 for the analysis. It allows comparing easily the results coming from the different discharges. Thus, there is no cavitation during experiments. The rise and fall results represent the two records for each discharge as explained in Section 5.1. Furthermore, the recirculation length (shown by the lower pressures downstream of the orifice in Figure 5) seems distinct from the discharge value as shown in [7].

Figure 6 shows the determination of the head loss coefficient with the least-square method for the 2^{nd} tested orifice.

According to Table 3, for the angle side approach (BA on Figure 1), the head loss coefficient decreases for angles between 0 and 30 degrees. For higher angles, head loss coefficient increases up to a 90-degrees angle (orifice with $\alpha = \alpha_i$ not tested in this study).

For the other side approach (AB on Figure 1), head loss coefficient increases immediately between 0 and 15 degrees to remain stable for higher angle (until 67 degrees).

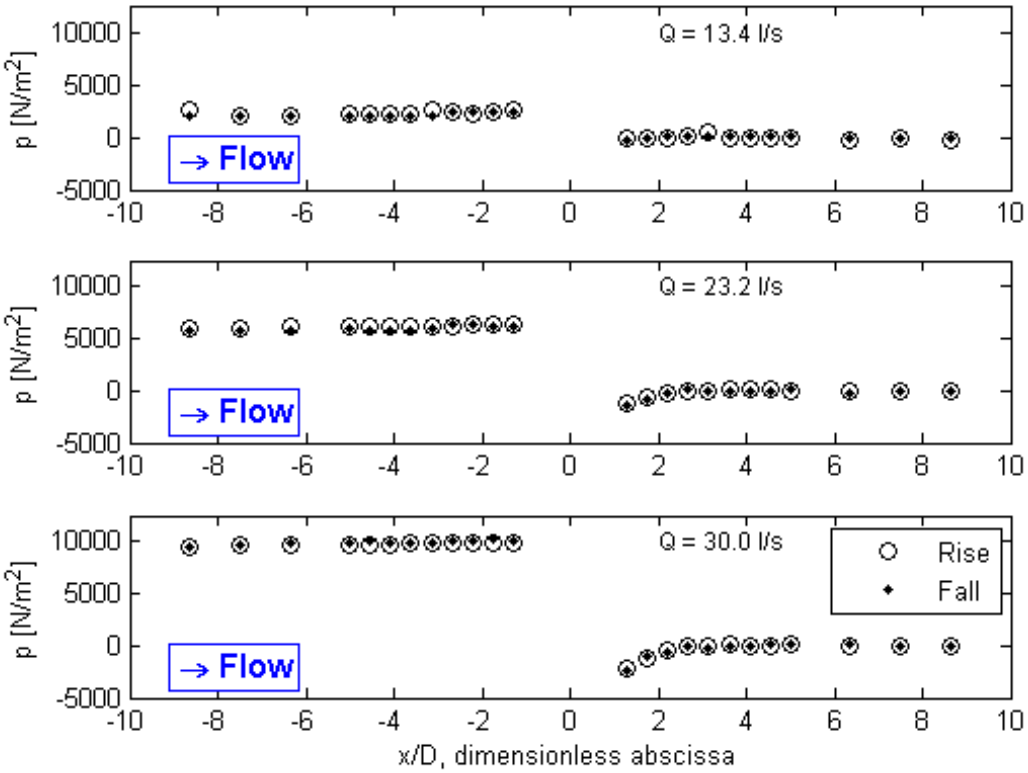

Figure 5. Pressure evolution along the main pipe axis for the orifice 1 ($\beta = 0.5$, $\alpha = 0.2$, $\alpha_i = 0.1$ and $\theta = 0°$) and flow direction AB (Three discharges 13.4, 23.2 and 30.0 l/s)

Table 3. Head loss coefficients k , coefficients of determination R^2 values and asymmetrical parameters

Experiment	k_{AB} [−]	R^2_{AB}	k_{BA} [−]	R^2_{BA}	$\frac{k_{BA}}{k_{AB}}$
1	24.8	0.9990	27.0	0.9971	1.08
2	30.7	0.9969	11.4	0.9956	0.37
3	30.5	0.9986	11.3	0.9889	0.37
4	29.6	0.9994	18.1	0.9964	0.61
5	31.1	0.9956	25.2	0.9995	0.81

The head loss ratio, $\frac{k_{BA}}{k_{AB}}$, shows the orifice asymmetrical behaviours. Logically, this ratio is as close to unity as possible for the first orifice ($\theta = 0$). However, it decreases significantly by almost 66% for smaller tested angles ($\theta \in [15, 30]$). Its value increases up to 81% for higher tested angles.

6.2. Numerical

First of all, the mesh quality is checked with the y^+ values. They are consistent with the wall treatment, i.e. wall function approach. Head losses found for the highest discharge (Table 2) by

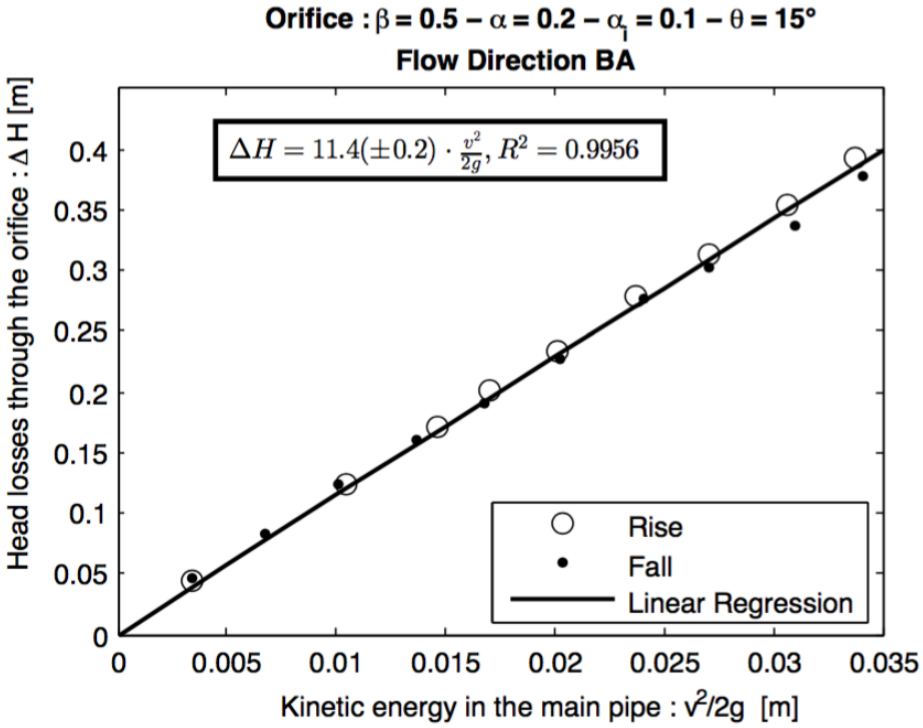

Figure 6. Head losses determination for orifice 2 ($\beta = 0.5$, $\alpha = 0.2$, $\alpha_i = 0.1$ and $\theta = 15°$) and flow direction BA

Table 4. Numerical head loss coefficients, y^+ values and asymmetrical parameters

Experiment	k_{AB} [−]	y^+_{AB}	k_{BA} [−]	y^+_{BA}	$\frac{k_{BA}}{k_{AB}}$
1	21.9	75.3	21.9	75.3	1.00
2	24.1	76.2	12.3	72.6	0.51
3	24.7	76.1	11.2	72.9	0.45
4	25.5	76.7	11.9	72.7	0.47
5	25.3	76.5	14.2	74.4	0.60

numerical model are shown in Table 4. In the same way as for physical results, the AB head losses increase by 10% with the presence of an angle and level off. On another way, the BA head losses decrease by almost 50% and increase again for higher angle.

Figure 7 to 10 show streamlines for orifice 1 and 2 for BA flow direction. It can be seen that the angle presence influences on the contraction and thus, the expansion of streamlines flowing through orifices. It can explain the difference and head loss decreasing for BA flow (Table 4).

6.3. Comparison

By Section 6.2 and 6.1 for BA flow, the numerical model is accurate enough only for small angles ($\theta \in [15°, 30°]$) but the maximum difference with physical results is almost 40% for higher discharge. For AB flow, the difference is about 20%.

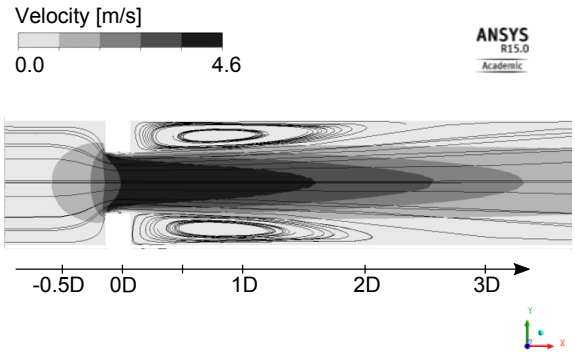

Figure 7. Streamline for orifice 1 ($\theta = 0°$) and $Q = 30\,l/s$

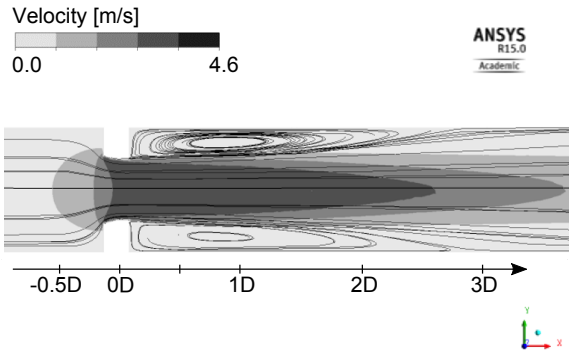

Figure 8. Streamline for orifice 2 ($\theta = 15°$) and $Q = 30\,l/s$

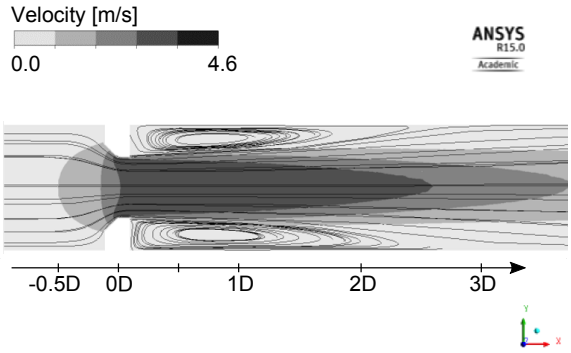

Figure 9. Streamline for orifice 3 ($\theta = 45°$) and $Q = 30\,l/s$

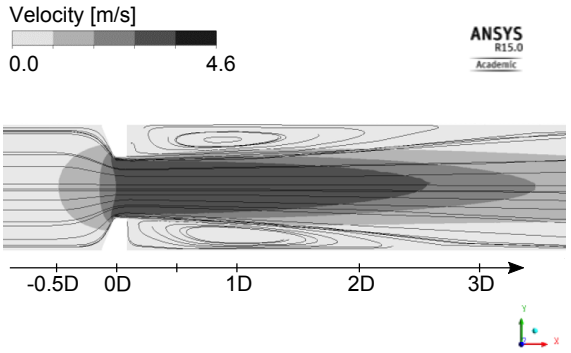

Figure 10. Streamline for orifice 4 ($\theta = 67°$) and $Q = 30\,l/s$

Figure 11 shows the pressure line along the pipe axis for orifice 2 for AB and BA flow direction (Table 1). While the upstream pressure head is not well reproduced by the numerical model, the downstream pressure follows quite well the downstream jet pressures.

These observations tend to show that the chosen turbulence model and mesh are not able to reproduce sudden geometry changes (like a 90° angle between two edges). However, when the change is smoother (here, for small sharp angles), numerical upstream pressures have better agreement with physical.

7. Conclusion

Two different ways are proposed to evaluate head losses produced by a given orifice with different sharp angle. Indeed, head losses depend largely on the orifice geometry in both direction.

Both approaches show that head loss asymmetry depend widely on the sharp angle values. For higher angles, the asymmetry decreases. However, this study shows that there are still large differences between physical and numerical results. These differences could come from the sudden geometry changes imposed by an orifice introduction.

Furthermore, physical experiments show that the introduction of an angle, even small, decreases significantly the losses in one flow direction while the other flow direction is relatively

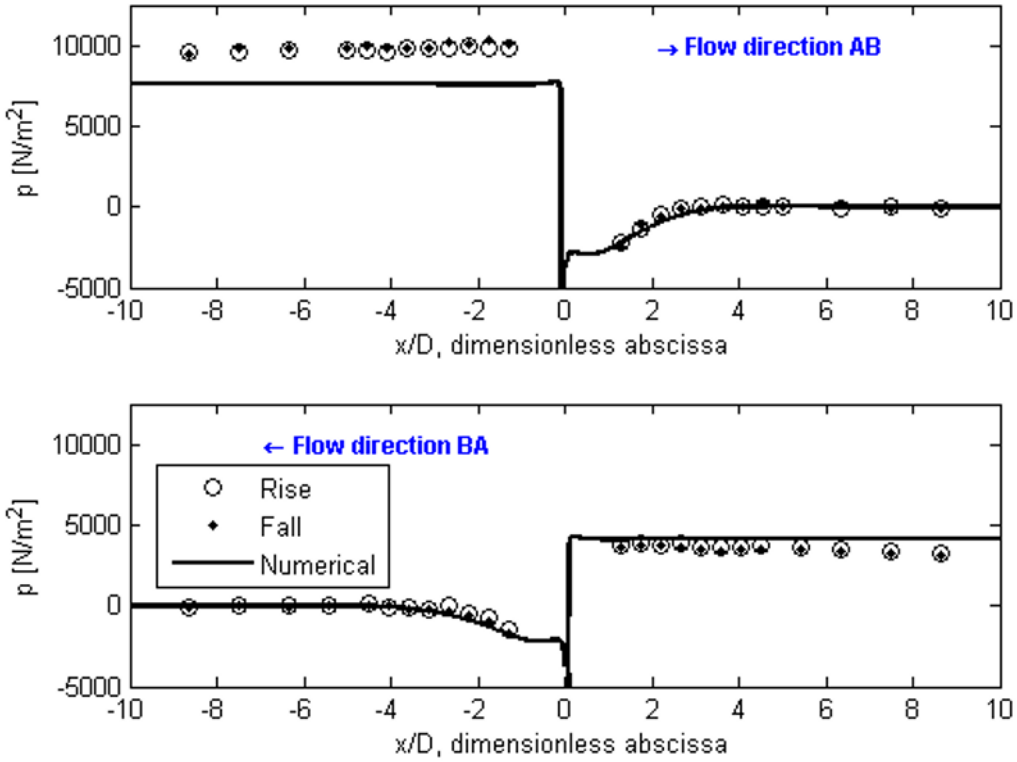

Figure 11. Pressure line for orifice 2 ($\beta = 0.5$, $\alpha = 0.2$, $\alpha_i = 0.1$ and $\theta = 15°$), $Q = 30\,l/s$ and for flow directions AB and BA

unaffected. The highest decreasing is almost 66% for angles between 15 and 30 degrees.

On the numerical side, future developments will be performed to improve the model accuracy. These developments will be the use of other turbulence models or meshing.

References

[1] De Cesare G, Adam N J, Nicolet C, Billeter P, Angermayr A and Valluy B 2015 Surge tank geometry modification for power increase (Bordeaux, France: The International Journal On Hydropower & Dams)

[2] Boillat J L and de Souza P 2004 *Hydraulic System - Modélisation des systèmes hydrauliques à écoulements transitoires en charge* Communiation LCH 16 (Ecole polytechnique fédérale de Lausanne: Ed. Anton Schleiss)

[3] Nicolet C 2007 *Hydroacoustic modelling and numerical simulation of unsteady operation of hydroelectric systems (Thesis 3751)* Ph.D. thesis

[4] International Standard 2003 Iso 5167-2 : Measurement of fluid flow by means of pressure differential devices inserted in circular cross-section conduits running full - part 2: Orifice plates

[5] Blevins R D 1984 *Applied fluid dynamics handbook* vol 1

[6] Idel'cik I 1969 *Mémento des pertes de charges singulières et de pertes de charges par frottement [Handbook of singular and friction head losses]*

[7] Jianhua W, Wanzheng A and Qi Z 2010 Head loss coefficient of orifice plate energy dissipator *Journal of Hydraulic Research* vol 48 pp 526–530